Check for updates

Risk Evaluation of EMT and Inflammation in Metastatic Pancreatic Cancer Cells Following Plasma Treatment

Eric Freund[1,2†], Chiara Spadola[2†], Anke Schmidt[1], Angela Privat-Maldonado[3], Annemie Bogaerts[3], Thomas von Woedtke[1,4], Klaus-Dieter Weltmann[1], Claus-Dieter Heidecke[2], Lars-Ivo Partecke[2,5], André Käding[2] and Sander Bekeschus[1*]

[1] ZIK plasmatis, Leibniz Institute for Plasma Science and Technology (INP), Greifswald, Germany, [2] Department of General, Visceral, Thoracic, and Vascular Surgery, Greifswald University Medical Center, Greifswald, Germany, [3] Plasma Lab for Applications in Sustainability and Medicine - ANTwerp, Department of Chemistry, University of Antwerp, Antwerp, Belgium, [4] Department of Hygiene and Environmental Medicine, Greifswald University Medical Center, Greifswald, Germany, [5] Schleswig Medical Hospital, Schleswig, Germany

The requirements for new technologies to serve as anticancer agents go far beyond their toxicity potential. Novel applications also need to be safe on a molecular and patient level. In a broader sense, this also relates to cancer metastasis and inflammation. In a previous study, the toxicity of an atmospheric pressure argon plasma jet in four human pancreatic cancer cell lines was confirmed and plasma treatment did not promote metastasis *in vitro* and *in ovo*. Here, these results are extended by additional types of analysis and new models to validate and define on a molecular level the changes related to metastatic processes in pancreatic cancer cells following plasma treatment *in vitro* and *in ovo*. In solid tumors that were grown on the chorion-allantois membrane of fertilized chicken eggs (TUM-CAM), plasma treatment induced modest to profound apoptosis in the tissues. This, however, was not associated with a change in the expression levels of adhesion molecules, as shown using immunofluorescence of ultrathin tissue sections. Culturing of the cells detached from these solid tumors for 6d revealed a similar or smaller total growth area and expression of ZEB1, a transcription factor associated with cancer metastasis, in the plasma-treated pancreatic cancer tissues. Analysis of *in vitro* and *in ovo* supernatants of 13 different cytokines and chemokines revealed cell line-specific effects of the plasma treatment but a noticeable increase of, e.g., growth-promoting interleukin 10 was not observed. Moreover, markers of epithelial-to-mesenchymal transition (EMT), a metastasis-promoting cellular program, were investigated. Plasma-treated pancreatic cancer cells did not present an EMT-profile. Finally, a realistic 3D tumor spheroid co-culture model with pancreatic stellate cells was employed, and the invasive properties in a gel-like cellular matrix were investigated. Tumor outgrowth and spread was similar or decreased in the plasma conditions. Altogether, these results provide valuable insights into the effect of plasma treatment on metastasis-related properties of cancer cells and did not suggest EMT-promoting effects of this novel cancer therapy.

Keywords: epithelial-to-mesenchymal transition, kINPen, plasma medicine, plasma sources, reactive oxygen species, ROS

INTRODUCTION

Cancer is the second leading cause of death worldwide after cardiovascular diseases [1]. Cancer incidence is increasing, and the spectrum of regionally dominating tumors and their mutational burden is heterogeneous. Hence, efficient cancer treatment remains challenging and is one of the significant difficulties of today. However, new concepts of cancer therapies are under investigation. This includes immunotherapies [2], target-specific drugs [3, 4], or technological innovations such as photodynamic [5, 6] and cold physical plasma therapy [7]. Cold physical plasmas are partially ionized gases generating a plethora of reactive species (ROS) besides other components such as electric fields, temperature, light of different wavelengths, and charged particles [8, 9]. At sufficient concentrations, these species mediate oxidation-induced damage and death in tumor cells [7]. Plasma treatment was previously shown to control tumor growth in pre-clinical models effectively [10–12]. Moreover, first patients with tumors of the head and neck benefited from this new therapeutic approach and experienced a reduced tumor burden [10, 11].

Today, increased tumor toxicity is only one of the columns of promising new cancer therapies. The other aspects include tolerability (beneficial ratio between anticancer activity and side effects) and safety aspects, for instance. Such risk assessment includes the investigations of whether a new treatment is void of inducing cancer cell detachment and metastasis. Metastasis is one of the greatest challenges in cancer therapies. Disseminated tumor growth induces organ dysfunction and often hinders surgical resection [12–15]. Especially in pancreatic cancer, the disseminated spread into the peritoneal cavity (peritoneal carcinomatosis) hinders successful cancer therapies [16–23]. Therefore, this type of cancer is a challenging but ideal model to investigate the effect of a novel treatment on cellular detachment and metastatic phenotype.

Treatments with the *kINPen* argon plasma jet had been shown to be void of genotoxicity according to OECD-based protocols [24–27] and did not introduce cell detachment through physical irritations (argon gas flow), or biological modulations of adhesion markers [28]. Moreover, the absence of tumor formation after six repetitive treatments of skin was validated in a 1-year follow up study in mice [26]. Also, clinicians that treated patients with the *kINPen* argon plasma jet in similar settings as investigated here (no modulation of feed- or sheath gases), did not report any severe side-effects [29–32]. This study now extends on the previous investigations of four different pancreatic cancer cell lines (MiaPaCa2, PaTuS, PaTuT, and Panc01) and tissue from *in ovo*-grown tumors, to a more detailed analysis of factors that can mediate an altered cell detachment and outgrowth. This includes (i) adhesion molecules, that are responsible for cell-cell and cell-matrix contact being essential to maintain tissue integrity [33–35], (ii) markers of the epithelial-mesenchymal transition (EMT), that are associated with cancer cell polarization and transformation to a more metastatic phenotype [18, 36, 37], and (iii) molecules of inflammation known to drive or limit inflammation-mediated cellular escape from the bulk tumor mass. In a series of experiments, it was demonstrated that the plasma treatment regime using the *kINPen* argon plasma jet was safe with respect to the aspects mentioned above and the model systems employed in this study. There were no hints for the promotion of EMT changes or metastasis and therefore further research in this field is strongly encouraged.

MATERIALS AND METHODS

Cell Cultivation and Plasma Treatment

The experiments were carried out with four human pancreatic cancer cell lines: MiaPaCa2 (ATCC: CRL-1420), PaTuS (DSMZ: ACC-162), PaTuT (DSMZ: ACC-204), and Panc01 (ATCC: CRL-1469). The culturing was performed in Dulbecco's modified Eagle's medium (DMEM; Pan Biotech, Aidenbach, Germany), which was supplemented with 10% fetal bovine serum, 2% glutamine, and 1% penicillin and streptomycin (all Sigma, Steinheim, Germany) in a cell culture incubator (Binder, Tuttlingen, Germany). For co-culture experiments, cells transduced with nuclear fluorescent proteins were used. The pancreatic stellate cell line RLT-PSC (developed at the Faculty of Medicine of the University of Mannheim [38], kindly provided by Prof. Ralf Jesenofsky) was transduced to express nuclear mKate2 (RLT-PSC Red) using a lentiviral vector (Essen BioScience, Essen, Germany). MiaPaCa2 (MiaPaCa2 Green) and Panc01 (Panc01 Green) were transduced to express nuclear green fluorescent protein (Essen BioScience, Essen, Germany). Cells were cultured in DMEM-F12 medium (Gibco, Dreieich, Germany). For experiments, absolute cell counting was performed using an Attune NxT flow cytometer (Thermo Scientific, Waltham, USA), and seeding was done in Roswell Park Memorial Institute medium 1640 (RPMI; Pan Biotech, Aidenbach, Germany) with similar supplements as for DMEM. For FACS experiments, 2×10^4 cells per well were seeded in 96-well flat-bottom plates (Eppendorf, Hamburg, Germany). For three-dimensional tumor spheroids, 3×10^3 cells per well in medium containing 0.24% Methocel (ratio 2:1, 2×10^3 RLT-PSC, 1×10^3 pancreatic cancer cells) were seeded in ultra-low attachment plates (Nunclon Sphera; Thermo Scientific, Waltham, USA). For seeding on the chorion allantois membrane of fertilized chicken eggs (TUM-CAM model), 2×10^6 cells were supplemented with 15 µl Matrigel (Corning, New York, USA). Before plasma treatment, the cells were cultured for an additional 24 h (FACS experiments), 72 h (spheroid experiments), and 96 h (TUM-CAM model). Plasma treatment was done using high-purity (99.999%) argon gas (Air Liquide, Paris, France) at two standard liters per minute running the atmospheric pressure argon plasma jet kINPen (neoplas tools, Greifswald, Germany). The plasma treatment of co-cultured spheroids (in 150 µl PBS and medium exchange 90 min later) was done for 120 s and standardized using an xyz-table (CNC Step, Gelfern, Germany), which fixed the plasma jet and operated the computer-driven treatment protocol.

In ovo Experiments

Specific pathogen-free chicken eggs (Valo BioMedia, Osterholz-Schrambeck, Germany) were incubated in an egg incubator (Thermo de Luxe 250, Hemel, Verl, Germany) at 37.5°C and

65% humidity at constant turning (for the first 6 days). The preparation of the eggs' chorion-allantois membrane (CAM) as well as the treatment was performed as described before [28]. Briefly, the tumor cells were implanted at day 8 of the incubation, and the plasma treatments were performed at days 12 and 14. The cell floaters were detached from the tumors by gently pipetting 150 µl of growth medium (RPMI) up and down and collecting the supernatant after the second plasma treatment. A part of the supernatant was stored for cytokine quantification, and the detached cell floaters were further incubated *in vitro* for the following 6 days (144 h). For this, flat-bottom 96-well cell culture plates (Eppendorf, Hamburg, Germany) were utilized that supply a ring which was filled with water to prevent excessive evaporation of culture medium during that time. After incubation, cells were subjected to imaging and flow cytometry analysis.

Tumor Tissue and Live-Cell Imaging

Tissues from the *in ovo* grown tumors were explanted from the CAM and embedded in OCT medium (Tissue-Tek; Sakura Fintek, Alphen aan de Rijn, Netherlands) before freezing in liquid nitrogen and storage at $-80°C$. Ultrathin tissue sections were cut (5 µm) and mounted (Dako fluorescence mounting medium; Agilent Technologies, Santa Clara, UA) on microscopy slides. For the quantification of apoptotic cells, the *In situ Cell Death Detection Kit* (TUNEL red; Roche, Basel, Switzerland) was utilized according to the manufacturer's instructions. For nuclear counterstaining, diamide-2-phenylindol (DAPI; BioLegend, San Diego, USA) was used. For the staining of cellular adhesion molecules, the tissue slides were fixed with 4% paraformaldehyde (PFA) and permeabilized with Triton-X (both Sigma Aldrich, St. Louis, USA). Blocking was performed with 5% bovine serum albumin (BSA; Sigma Aldrich, St. Louis, USA) before they were stained with the respective antibodies targeting CD49b conjugated with phycoerythrin (PE; clone: P1E6-C5; BioLegend, San Diego, USA), CD326 conjugated with AlexaFluor (AF) 488 (clone: 9C4; BioLegend, San Diego, USA), and CD324 conjugated with AF647 (clone: EP700Y; Abcam, Cambridge, UK). The images were acquired using a BZ-9000 fluorescence microscope (Keyence, Frankfurt, Germany). The ratio of TUNEL+ cells over the area of the tissue region was quantified utilizing the image analysis software ImageJ.

For the investigation of cultured *ex ovo* tumor cell floaters, and *in vitro* grown three-dimensional tumor and pancreatic stellate cell spheroids, high content imaging was performed utilizing the Operetta CLS imaging system (PerkinElmer, Waltham, USA). The *ex ovo* floaters were fixed and permeabilized as described above and were imaged with a 20 × air objective (NA = 0.4; Carl Zeiss, Jena, Germany) acquiring brightfield as well as fluorescence images at λ_{ex} 365 nm and λ_{em} 430–500 nm for the detection of DAPI, and λ_{ex} 630 nm and λ_{em} 655–760 nm for the detection of Zinc finger E-box-binding homeobox 1 (anti-ZEB1 AF700, clone: 639914, R&D Systems / biotechne, Minneapolis, USA). For the algorithm-driven (Harmony 4.9; PerkinElmer, Waltham, USA) image and cell quantification strategy, a pseudo-fluorescence channel was calculated by merging the fluorescence channels. The total cellular proliferation area resulting from

the initial cell floaters added as well as the ZEB1 fluorescence intensity inside that growth area was calculated. The three-dimensional tumor and stellate cell spheroids were imaged 72 h after their treatment with plasma. This was done utilizing a 5 × objective (NA 0.16; Carl Zeiss, Jena, Germany) capturing the brightfield channel, as well as the fluorescence channels for the detection of GFP-expressing tumor cells at λ_{ex} 475 nm and λ_{em} 500–550 nm, and for mKate-expressing stellate cells at λ_{ex} 560 nm and λ_{em} 570–650 nm. The detection of the spheroid area was done by creating a pseudo fluorescence image out of the merged fluorescent channels and an inverted brightfield image, which had the highest intensities in the area of spheroid growth. The cell outgrowth was calculated by determining the number of cells outside the spheroid region. Their distance to the spheroid border region was calculated automatically based on algorithms implemented in the quantitative imaging software.

Flow Cytometry

To quantify the expression of adhesion molecules and markers of the epithelial-to-mesenchymal transition (EMT), the cells were treated in 96-well flat-bottom plates and were harvested 24 h later with accutase (Pan Biotech, Aidenbach, Germany). Subsequently, the cells were transferred to a u-bottom plate (Nunclon; Thermo Scientific, Waltham, USA) and were fixed and permeabilized. The cells were stained with DAPI and antibodies targeting αSMA conjugated with AF594 (clone: 1A4; Abcam, Cambridge, UK), anti-vimentin conjugated with PerCP/Cy5.5 (clone: H84; Santa Cruz Biotechnology Dallas, USA), and anti-ZEB1 conjugated with AF700 (clone: 639914; R&D Systems, Minneapolis, USA). After washing, cells were acquired with a Cytoflex S (Beckman-Coulter, Brea, USA) flow cytometer. The expression of the markers was quantified in viable (DAPI−) cells and normalized to that of untreated cells. Unstained controls were treated like their counterparts and were acquired using the same settings. Data analysis was done using Kaluza 2.1 (Beckman-Coulter, Brea, USA).

Quantitative Polymerase Chain Reaction (qPCR)

The cell lines were cultured in optimal growing conditions before they were harvested with the enzyme accutase, and cell pellets were generated via centrifugation and washing of the cells. Afterward, they were suspended in lysis buffer, and cellular RNA was isolated utilizing an isolation kit according to the manufacturers' instructions (RNA Mini Kit; Bio&SELL, Feucht, Germany). The RNA was quantified using a NanoDrop 2000C (Thermo Scientific, Waltham, MA, USA). Quantitative polymerase chain reaction (qPCR) was then carried out with 1 µg RNA that was synthesized into cDNA using a thermocycler device (Thermo Scientific, Waltham, USA). For these experiments, 96-well v-bottom plates loaded with Sybr Green (BioRad, Munich, Germany) were used to label the mRNA-targets during 50 heat cycles (Light Cycler 480; Roche, Mannheim, Germany). Expression levels were calculated with formulas provided by the $2^{-\Delta\Delta Ct}$ method and in relation to *GAPDH*.
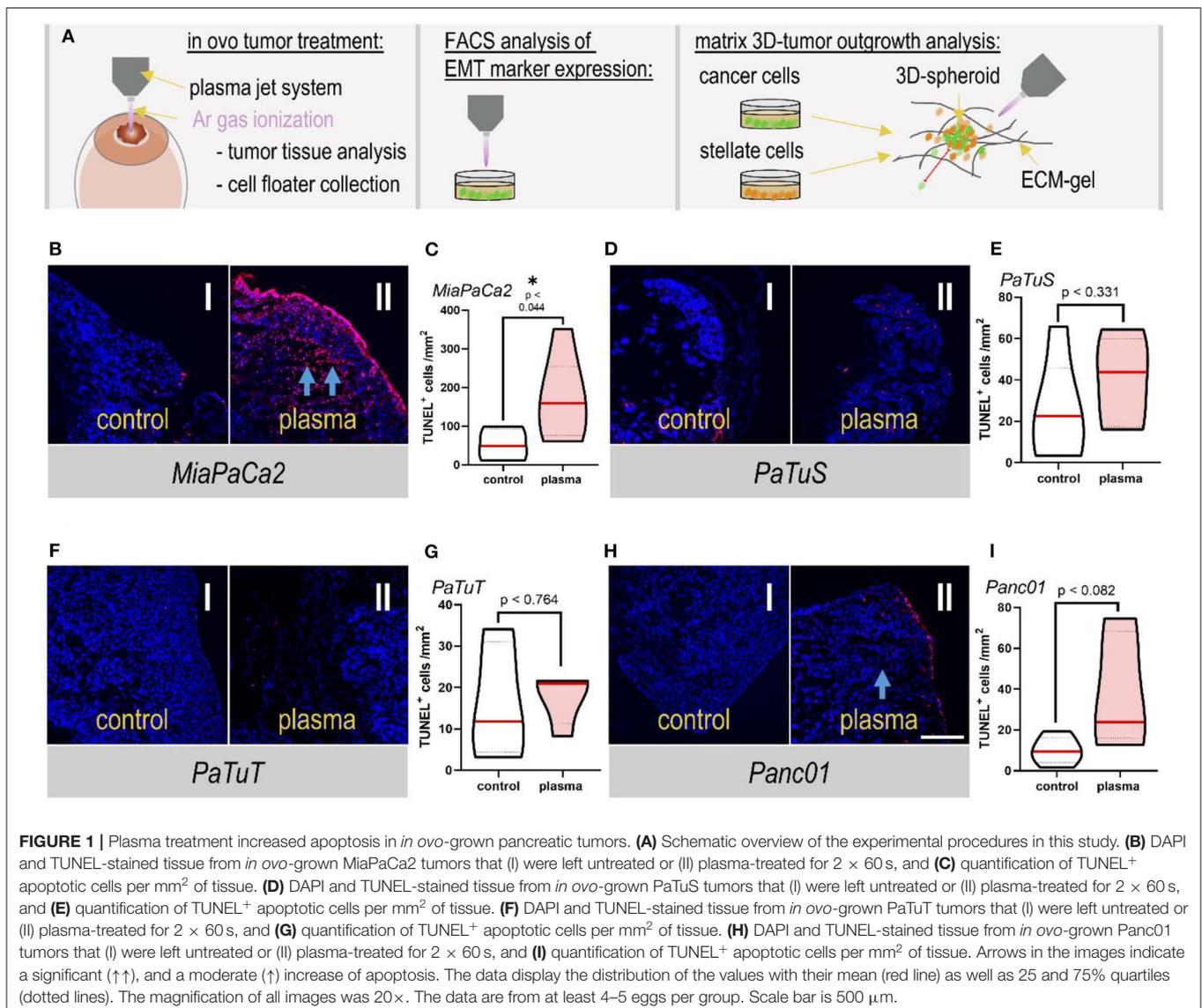
Quantification of Chemokine/Cytokines

Supernatants for chemokine/cytokine analysis of cancer cells were collected 4 h post-treatment of the *in vitro* experiments 96-well plates as well as 30 min after plasma treatment of TUM-CAM with subsequent rinsing of tumors and aspiration of the liquid. Supernatants were stored in 96-well plates at −80°C. For detection of the soluble inflammatory mediators (chemokines/cytokines), the LEGENDplex (BioLegend, San Diego, USA) bead-based immunoassay was utilized. The experiments were carried out according to the manufacturer's instructions. The targets of the assay were the following: interleukin (IL) 1β, IL6, IL8, IL10, and IL12p70, free-active tumor growth factor β (TGFβ), tumor necrosis factor α (TNFα), interferon γ (IFNγ), C-X-C motif chemokine ligand 1(CXCL1), CXCL10, arginase, C-C motif ligand 17 (CCL17/TARC), and vascular endothelial growth factor (VEGF). All 13 targets were quantified simultaneously, each with specific standards and limits

of detection. Staining and measurement of samples were done in v-bottom 96-well plates (Eppendorf, Hamburg Deutschland), from which the fluorescent beads were directly acquired with a flow cytometer (CytoFlex; Beckman Coulter, Brea, USA). The discrimination between the 13 different beads was done using differences in forward and side scatter (FSC, SSC) and fluorescent intensity at λ_{ex} 638 nm and λ_{em} 640–680 nm. By analyzing the fluorescence intensity of PE-labeled antibodies (λ_{ex} 561 nm and λ_{em} 564–606 nm) detecting the targets bound to the beads, the absolute concentration of all factors was interpolated using polynomial functions of the 5th degree and dedicated data analysis software (Vigene Tech, Carlisle, USA).

Statistical Analysis

Data are from two to six experiments with several technical replicates. For statistical analysis and graphing, Prism 8.4.2 (GraphPad, San Diego, USA) was utilized. Multiple comparisons

FIGURE 1 | Plasma treatment increased apoptosis in *in ovo*-grown pancreatic tumors. **(A)** Schematic overview of the experimental procedures in this study. **(B)** DAPI and TUNEL-stained tissue from *in ovo*-grown MiaPaCa2 tumors that (I) were left untreated or (II) plasma-treated for 2 × 60 s, and **(C)** quantification of TUNEL+ apoptotic cells per mm2 of tissue. **(D)** DAPI and TUNEL-stained tissue from *in ovo*-grown PaTuS tumors that (I) were left untreated or (II) plasma-treated for 2 × 60 s, and **(E)** quantification of TUNEL+ apoptotic cells per mm2 of tissue. **(F)** DAPI and TUNEL-stained tissue from *in ovo*-grown PaTuT tumors that (I) were left untreated or (II) plasma-treated for 2 × 60 s, and **(G)** quantification of TUNEL+ apoptotic cells per mm2 of tissue. **(H)** DAPI and TUNEL-stained tissue from *in ovo*-grown Panc01 tumors that (I) were left untreated or (II) plasma-treated for 2 × 60 s, and **(I)** quantification of TUNEL+ apoptotic cells per mm2 of tissue. Arrows in the images indicate a significant (↑↑), and a moderate (↑) increase of apoptosis. The data display the distribution of the values with their mean (red line) as well as 25 and 75% quartiles (dotted lines). The magnification of all images was 20×. The data are from at least 4–5 eggs per group. Scale bar is 500 μm.

were done with ANOVA (with Welch's correction). For comparison between two adjacent groups, the Welch's t-test was used. The levels of significance are indicated in the figures as asterisks: $\alpha = 0.05$ (*), $\alpha = 0.01$ (**), and $\alpha = 0.001$ (***).
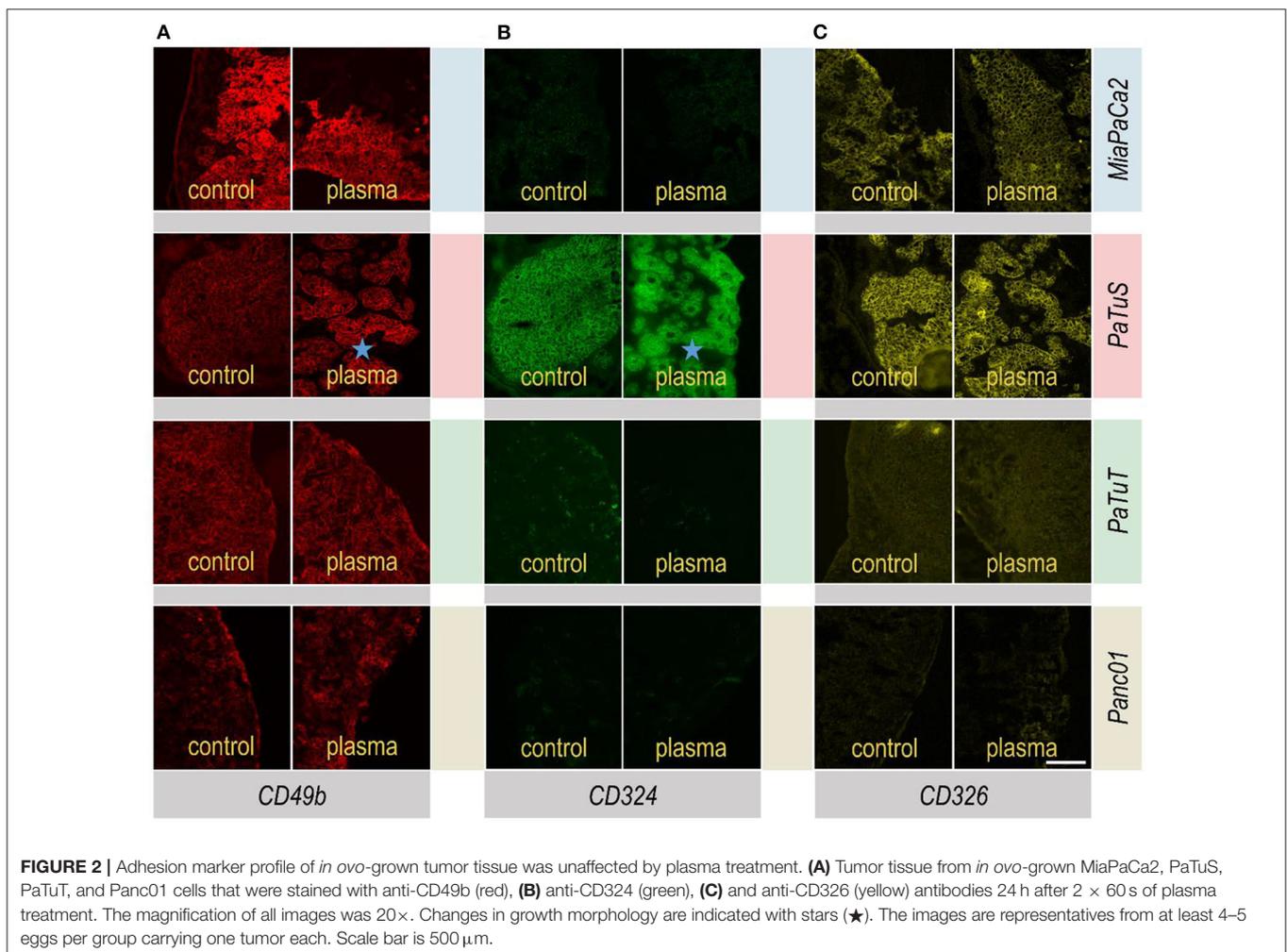
RESULTS

Plasma Treatment Partly Elicited Apoptosis of Pancreatic Cancer Cells Grown *in ovo*
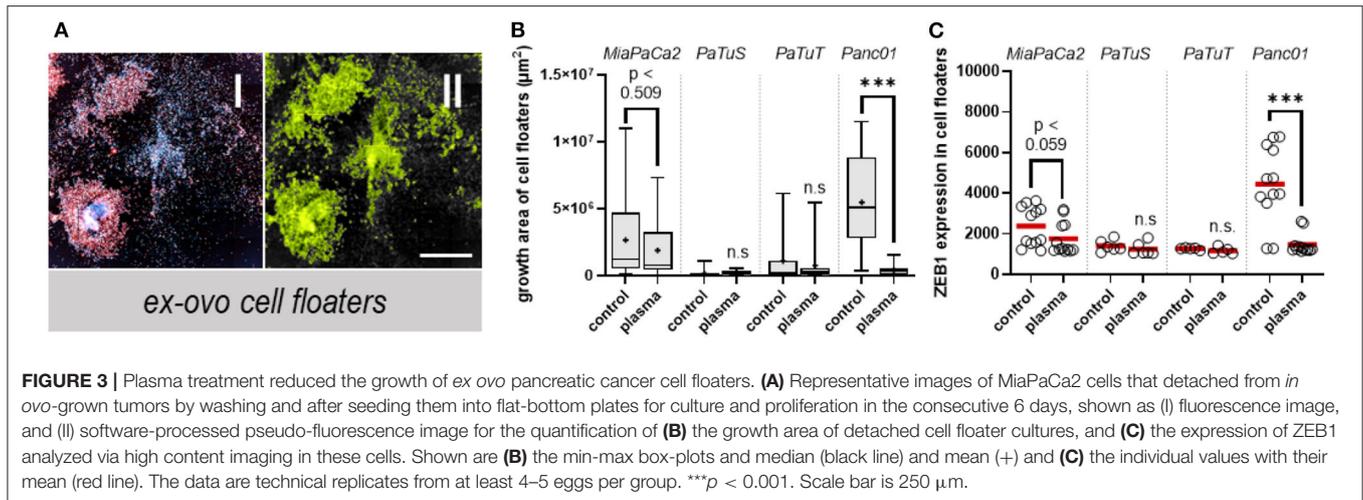
To test the anticancer efficacy of cold physical plasma generated via the kINPen, different pancreatic cancer cell lines (MiaPaCa2, PaTuS, PaTuT, and Panc01) were seeded on the chorion-allantois membrane of fertilized chicken eggs (TUM-CAM model) to grow solid tumors before these were plasma-treated twice for 60 s on two consecutive days (**Figure 1A**). The induction of apoptosis was different among the cell lines tested. A significant effect ($p < 0.044$) of plasma treatment was observed in MiaPaCa2 tumors (**Figures 1B,C**). An apparent increase in the apoptosis rate (TUNEL$^+$ cells) was visible in the tumor surface region, and to a lower amount also in deep tissue layers (**Figure 1B**). In contrast, PaTuS cells did not show large rates of apoptosis

after plasma treatment ($p < 0.764$; **Figures 1D,E**). Similar results were obtained for PaTuT cells ($p < 0.331$) (**Figures 1F,G**). For Panc01 tumors, a modest increase ($p < 0.082$) of apoptotic cells was observed in the plasma treatment conditions, especially at the tumor margins (**Figures 1H,I**).

Plasma Treatment Did Not Affect the Adhesion Marker Profile of *in ovo*-Grown Tumors

Cellular adhesion is a critical factor in tumor metastasis. In addition to the mechanical spread of tumor cells through invasive measures, endogenous metastasis occurs when cells actively detach from their mass and migrate into blood vessels and lymph nodes. Therefore, the expression of adhesion molecules in untreated and plasma-treated tumors was investigated. Tissue sections were prepared, and tissue slides were stained for the cell adhesion markers integrin alpha-2 (CD49b; **Figure 2A**), E-cadherin (CD324; **Figure 2B**), and Ep-CAM (CD326; **Figure 2C**). It was found that CD49b was expressed across all different tumor cell lines, albeit to a different extent. CD324 was highly expressed only in PaTuS but not in the three

FIGURE 2 | Adhesion marker profile of *in ovo*-grown tumor tissue was unaffected by plasma treatment. **(A)** Tumor tissue from *in ovo*-grown MiaPaCa2, PaTuS, PaTuT, and Panc01 cells that were stained with anti-CD49b (red), **(B)** anti-CD324 (green), **(C)** and anti-CD326 (yellow) antibodies 24 h after 2 × 60 s of plasma treatment. The magnification of all images was 20×. Changes in growth morphology are indicated with stars (★). The images are representatives from at least 4–5 eggs per group carrying one tumor each. Scale bar is 500 μm.

FIGURE 3 | Plasma treatment reduced the growth of *ex ovo* pancreatic cancer cell floaters. **(A)** Representative images of MiaPaCa2 cells that detached from *in ovo*-grown tumors by washing and after seeding them into flat-bottom plates for culture and proliferation in the consecutive 6 days, shown as (I) fluorescence image, and (II) software-processed pseudo-fluorescence image for the quantification of **(B)** the growth area of detached cell floater cultures, and **(C)** the expression of ZEB1 analyzed via high content imaging in these cells. Shown are **(B)** the min-max box-plots and median (black line) and mean (+) and **(C)** the individual values with their mean (red line). The data are technical replicates from at least 4–5 eggs per group. ***$p < 0.001$. Scale bar is 250 μm.

other tumor cell lines. CD326 expression was found in MiaPaCa2 and PaTuS tumors, but only to a negligible extent in PaTuT and Panc01 tumors. Interestingly, the growth pattern of PaTuS tumors was changed following the treatment with plasma to a more glandular, epithelial phenotype. A decrease in E-cadherin and Ep-CAM is a known indicator of pro-metastatic cancer phenotypes, suggesting plasma treatment not to interfere with such processes.
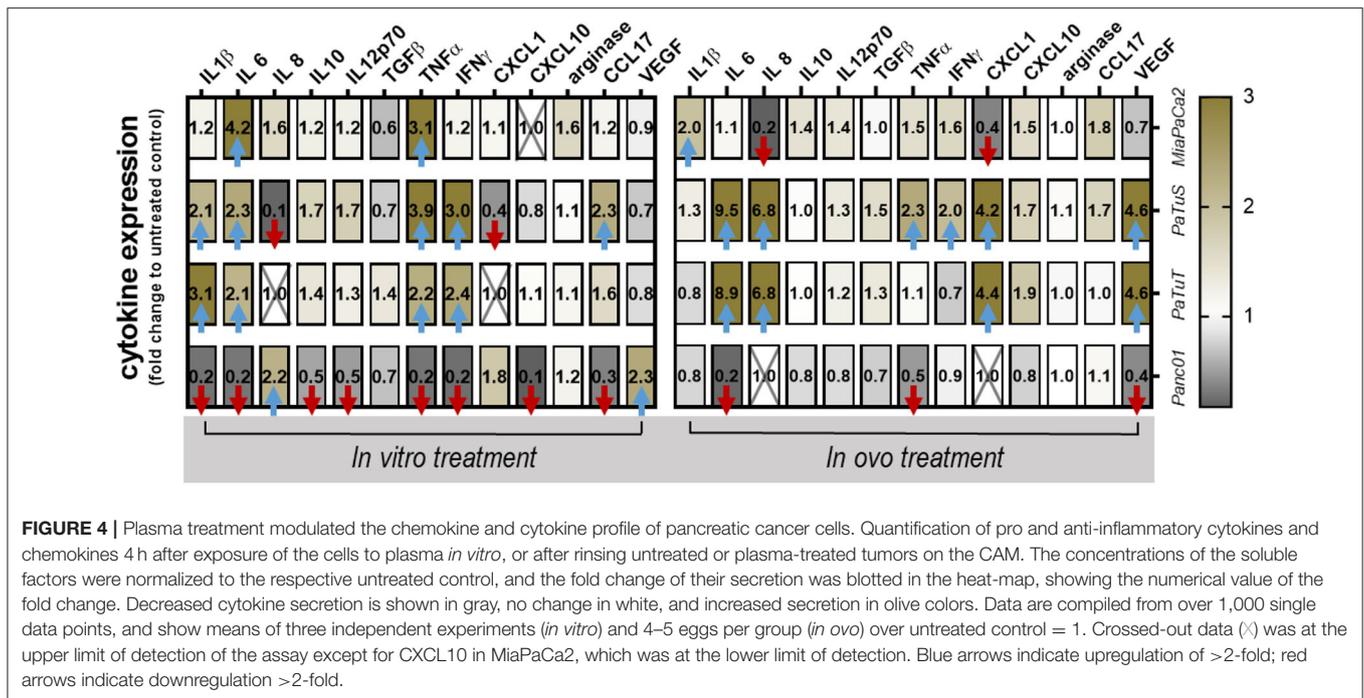
Plasma Treatment Neither Promoted Cell Detachment Nor Expression of ZEB1

After analyzing the toxicity and adhesion-related receptor expression in solid pancreatic cancer tissue, the next question was whether plasma treatment actively engaged the dislodgement of individual cells from the main tumor. This might occur due to, e.g., argon gas pressure, electrical discharges, drying of the outer tumor surface, and ROS-mediated breakage of cell-cell connections. The experiment was done by plasma treatment of the tumors and washing the tumors immediately afterward. The cells that were contained in the washing solution (cell culture medium) were then seeded into cell culture plastic and allowed to grow for 6 days (144 h). This was necessary, as the number of cells retrieved directly in the washing solution was too low to perform intelligent imaging analysis. After 6 days, the cell growth was calculated using a software-based method that was utilizing a filtered image to detect the area of these cell floaters (**Figure 3A**). In MiaPaCa2 cells, it was found that the cell growth non-significantly decreased with plasma treatment, while PaTuS and PaTuT cells contained in the washing liquid overall failed to proliferate significantly *in vitro* (**Figure 3B**). In both cell lines, the growth area was similar or smaller in the plasma treatment condition. This does not suggest that these cells do not grow *in vitro*, but rather the cells detached from the original tumor mass were mostly not viable or too low in numbers. Panc01 cells, in contrast, had a large growth area in the control group, which significantly declined in the plasma treatment group (**Figure 3B**). These results suggest that plasma treatment either did not promote the detachment of pancreatic

tumor cells from the bulk tumor mass or that detachment was promoted, but the cells were dead, unable to proliferate, or both. The next question was whether the cells that grew *in vitro* changed their expression levels of the zinc finger e-box binding homeobox 1 (ZEB1) transcription factor, known to be associated with the mesenchymal transition of cancer cells [18]. ZEB1 was detected in the highest amount in MiaPaCa2 and Panc01 cells, and both of these cell lines showed a reduction of ZEB1 expression in the cells initially detached from the plasma-treated bulk tumor mass (**Figure 3C**), suggesting a decreased EMT phenotype.

Plasma Treatment Modulated the Inflammatory Profile *in vitro* and *in ovo*

Inflammation is one key aspect in tumor metastasis, and cytokines and chemokines are the major regulators of inflammation. Therefore, 13 different soluble mediators of inflammation were quantified in supernatants of *in vitro* and *in ovo* experiments (**Figure 4**). All data were normalized to that of untreated controls, while crossed out boxes indicate concentrations above or below the detection limit of the assay. Arrows indicate a 2-fold up or downregulation. Three is an only partial agreement between the *in vitro* and *in vivo* results, exemplifying the need to address research questions in both systems. Panc01 showed a consistent downregulation of almost all cytokines investigated *in vitro* and *in ovo*, except VEGF and IL8. By contrast, *in vitro* supernatant analysis of MiaPaCa2 and PaTuT revealed only upregulation of cytokines for IL6 and TNFα in both cell lines, and IL1β and TNFα in MiaPaCa2. The results for PaTuS were mainly analogous to those retrieved for PaTuT, except for an increase in CCL17 and a decrease in IL8 and CXCL1. While some of the results were similar to those seen in the *in ovo* samples (e.g., for IL6 and TNFα), some were different either in amplitude or direction of regulation. This was expected, as the CAM provided a nutritious and vascularized tumor microenvironment in which the cells modulate the expression of several genes associated with, e.g., extracellular matrix generation, differentiation, and

FIGURE 4 | Plasma treatment modulated the chemokine and cytokine profile of pancreatic cancer cells. Quantification of pro and anti-inflammatory cytokines and chemokines 4 h after exposure of the cells to plasma *in vitro*, or after rinsing untreated or plasma-treated tumors on the CAM. The concentrations of the soluble factors were normalized to the respective untreated control, and the fold change of their secretion was blotted in the heat-map, showing the numerical value of the fold change. Decreased cytokine secretion is shown in gray, no change in white, and increased secretion in olive colors. Data are compiled from over 1,000 single data points, and show means of three independent experiments (*in vitro*) and 4–5 eggs per group (*in ovo*) over untreated control = 1. Crossed-out data (✕) was at the upper limit of detection of the assay except for CXCL10 in MiaPaCa2, which was at the lower limit of detection. Blue arrows indicate upregulation of >2-fold; red arrows indicate downregulation >2-fold.
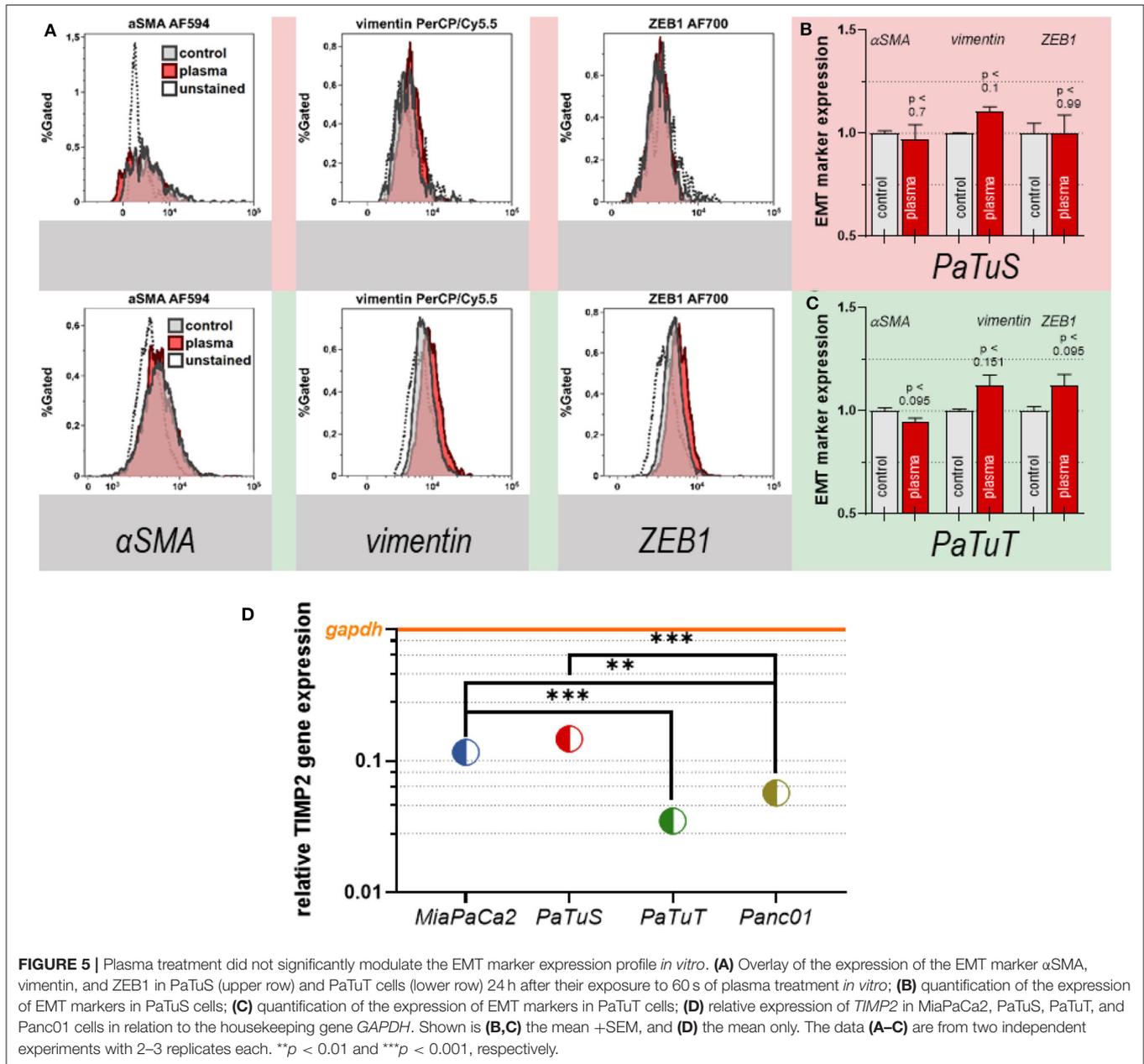
angiogenesis. In general, it was observed that PaTuS and PaTuT cells showed a similar pattern in the secretion of IL6, IL8, CXCL1, and VEGF *in vitro* and *in ovo*, which validates their similar nature.

Plasma Treatment Did Not Induce an EMT Phenotype in Pancreatic Cancer Cells *in vitro*

PaTuT and PaTuS cells only showed few cell detachment in the *in ovo* experiments. However, they had the most vital changes in cytokine expression among the tested cancer cell lines. Hence, it was tested if the plasma treatment induced a more invasive mesenchymal phenotype (EMT) that is associated with tumor cell metastasis and growth. The expression of α-smooth-muscle actin (αSMA), was unaffected, while vimentin was slightly increased ($p < 0.1$; **Figures 5A,B**) in PaTuS cells. ZEB1 was not found to be expressed in PaTuS cells (**Figures 5A,B**). In PaTuT cells, α SMA did not show any change in the cells after exposure to plasma (**Figures 5A,C**). Vimentin and ZEB1 gave a modest, non-significant upregulation after plasma treatment (**Figures 5A,C**). Another marker that is protective against tumor invasion and angiogenesis is the Tissue inhibitor of metalloproteinases 2 (TIMP2) [39]. Therefore, the expression of *TIMP2* was investigated among all pancreatic cancer cell lines that were tested in this study. PaTuS cells showed the highest gene expression of *TIMP2*, followed by MiaPaCa2. The expression in both of the cell lines was significantly different compared to PaTuT and Panc01 cells, which had low levels of *TIMP2* (**Figure 5D**).

Plasma Treatment Reduced the Cancer Cell Outgrowth in a Stellate Cell-Matrix-3D-Model

To provide a tumor microenvironment that could be monitored via fluorescence microscopy, a co-culture of human pancreatic stellate and cancer cells was setup. The former are myofibroblasts contributing to matrix formation and remodeling. The 3D tumor spheroid mixtures were exposed to plasma and embedded into a basement membrane matrix (growth factor reduced Matrigel) containing mainly laminin and vimentin collagens providing growth conditions for the cells [34] that allow the analysis of the evasion of the fluorescently labeled cells from the bulk tumor over time using quantitative multicolor fluorescence live-cell microscopy. MiaPaCa2 and Panc01 cells showed the highest release of floaters that had detached from the bulk tumor and grown *in vitro* (**Figure 3B**). Therefore, these two cell lines were used in this model as we expected a high degree of motility. Plasma treatment reduced the size area of the core spheroid in both cancer cell types co-cultured with stellate cells (**Figure 6A**). Interestingly, the stellate cells had a higher capacity of exiting the core spheroid into the extracellular matrix (**Figures 6B,E**, orange cells). Quantification of the absolute number (**Figure 6C**) of evaded cells and absolute distance of evaded cells to the spheroid core (**Figure 6D**) in the stellate cell-MiaPaCa2 spheroid model showed no significant difference for both cell types. By contrast, both the number of cells (**Figure 6F**) as well as their mean migration distance (**Figure 6G**) significantly decreased with plasma treatment of Panc01 cells co-cultured with stellate cells in 3D spheroids.
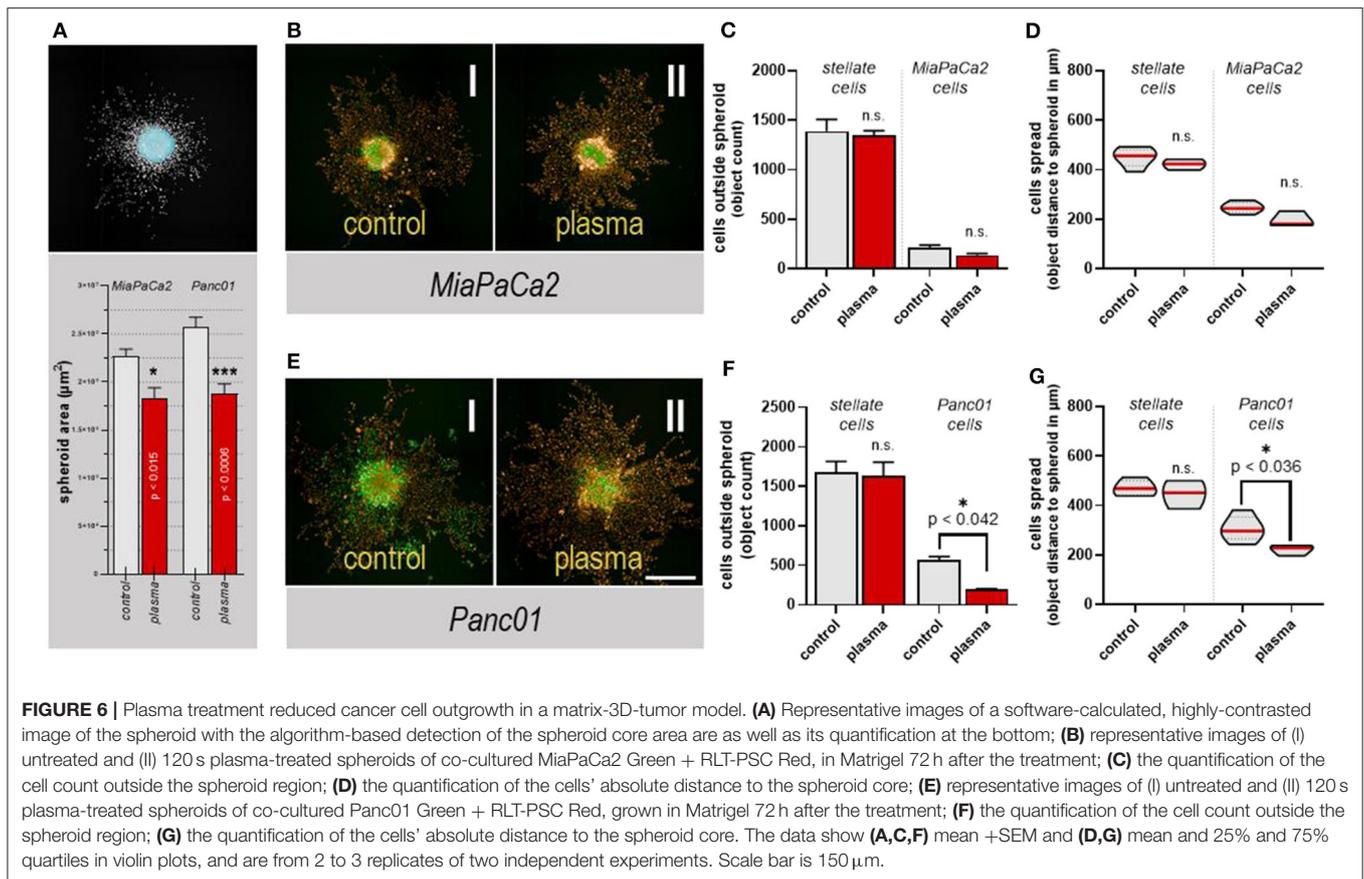
FIGURE 5 | Plasma treatment did not significantly modulate the EMT marker expression profile *in vitro*. **(A)** Overlay of the expression of the EMT marker αSMA, vimentin, and ZEB1 in PaTuS (upper row) and PaTuT cells (lower row) 24 h after their exposure to 60 s of plasma treatment *in vitro*; **(B)** quantification of the expression of EMT markers in PaTuS cells; **(C)** quantification of the expression of EMT markers in PaTuT cells; **(D)** relative expression of *TIMP2* in MiaPaCa2, PaTuS, PaTuT, and Panc01 cells in relation to the housekeeping gene *GAPDH*. Shown is **(B,C)** the mean +SEM, and **(D)** the mean only. The data **(A–C)** are from two independent experiments with 2–3 replicates each. **p < 0.01 and ***p < 0.001, respectively.

DISCUSSION

Pancreatic cancer is an aggressive and fast-growing tumor entity [40, 41]. It is often diagnosed at very late stages after there are already metastases in the liver or lungs. Peritoneal metastases may also be present at this time [41, 42]. Even with surgery in a resectable tumor, the number of R0 resections (no tumor tissue in the respective margins) remains to low [43, 44]. Pancreatic cancer has a poor prognosis, and the importance of cell residuals is outlined by the median survival that drops from 25.1 months (for R0) to only 15.3 months with R1 resection [16]. A combination with plasma treatment might become an additive approach to existing surgical and chemotherapeutic strategies to tackle the tumor cell residuals at the surgical margins of the pancreas.

Additional treatment of these cancer cell residuals might be able to decelerate the rapid course of cancer remission observed in most patients. Plasma treatment showed promising effects against pancreatic cancer cells *in vitro* [45–48] and *in vivo* [49–52]. However, the possibility of inducing a more metastatic phenotype in the cells surviving the treatment is underexplored. Early studies with experimental plasma jets showed an increase in cellular detachment [53–55]. Recent investigations did not report any cellular detachment in the TUM-CAM or spheroid model [28, 34], or a lack of EMT marker modulation after cellular exposure to plasma-oxidized medium [23].

In our previous work, it was shown that plasma treatment introduced cellular toxicity *in vitro* and reduced the tumor mass of tumors grown on the chorion-allantois membrane of fertilized

FIGURE 6 | Plasma treatment reduced cancer cell outgrowth in a matrix-3D-tumor model. **(A)** Representative images of a software-calculated, highly-contrasted image of the spheroid with the algorithm-based detection of the spheroid core area are as well as its quantification at the bottom; **(B)** representative images of (I) untreated and (II) 120 s plasma-treated spheroids of co-cultured MiaPaCa2 Green + RLT-PSC Red, in Matrigel 72 h after the treatment; **(C)** the quantification of the cell count outside the spheroid region; **(D)** the quantification of the cells' absolute distance to the spheroid core; **(E)** representative images of (I) untreated and (II) 120 s plasma-treated spheroids of co-cultured Panc01 Green + RLT-PSC Red, grown in Matrigel 72 h after the treatment; **(F)** the quantification of the cell count outside the spheroid region; **(G)** the quantification of the cells' absolute distance to the spheroid core. The data show **(A,C,F)** mean +SEM and **(D,G)** mean and 25% and 75% quartiles in violin plots, and are from 2 to 3 replicates of two independent experiments. Scale bar is 150 μm.

chicken eggs (TUM-CAM *in ovo* model) [28]. The TUM-CAM model provides a realistic setting for the growth of solid tumors. It supplies an extracellular matrix, as well as a supply of blood and nutrients through the chicken embryo's blood vessels [56]. Argon gas flow alone did not alter the metabolic activity of the tested cancer cell in the same setting, and more importantly, did also not significantly detach cells from the *in ovo* grown tumors. The role of mechanical stress that is applied through a similar plasma treatment can therefore be neglected, indicating the changes in EMT and adhesion marker profile to be more important for the initiation of metastasis. These investigations were now expanded to further downstream analysis of the tumor tissue. Despite a modest to substantial induction of apoptosis in plasma-treated tumor tissue, a change in some of the main cell adhesion molecules was not observed. Cells, including tumor cells, usually firmly adhere to the bulk mass via adhesion molecules, such as CD49b (integrin α-2), CD324 (E-cadherin), and CD326 (Ep-CAM) [15, 28, 57–59].

CD49b is an integrin involved in cellular contacts with laminin and collagen of extracellular matrices. Early work reported MiaPaCa2 cells to be void of CD49b [60], but similar to other studies [28] we found the molecule to be expressed in these and all other cell types. Ep-CAM plays a controversial role in the progression of epithelial tumors. This molecule is an adhesion molecule often found to be overexpressed in non-malignant epithelial. CD326 is also associated with tumor cell signaling (mandatory function in tumor cell invasion) and is–because of

its higher expression in cancers—described as a tumor-antigen [61, 62]. Novel therapy approaches also use targeted-therapies against Ep-CAM to prevent tumor growth [63]. However, Ep-CAM was only found expressed in tissue from MiaPaCa2 and PaTuS tumors and was not modulated by their treatment with plasma. Cell-cell contacts are mediated via E-cadherin (CD324), which has a crucial function in preserving tissue stability [58]. Reduced expression or loss of CD324 is associated with a more motile, invasive cancer cell phenotype [64]. In our study, CD324 was only expressed in PaTuS and in PaTuT cells to a modest extent. This corresponds to our finding that both cell lines released the lowest number of viable floaters from *in ovo*-grown tumors to proliferate *in vitro*. MiaPaCa2 and Panc01 cells showed only background level of E-cadherin staining in tumor tissues. Subsequently, they showed more *in vitro* growth from cellular floaters initially detached from the *in ovo*-grown tumor. Importantly, plasma treatment reduced the amount of MiaPaCa2 and Panc01 cells grown *in vitro* after *in ovo* treatment of tumors. Similar findings were made for ZEB1 expression levels in the *in vitro* cultures. ZEB1 is a transcription factor highly associated with tumor progression and metastasis [65]. It is known that this factor is associated with EMT in pancreatic cancer and leads to signaling cascades changing the cellular polarity and reducing the expression of adhesion markers such as E-cadherin [18, 66, 67]. It is also associated with decreased prognosis in various types of tumors [68]. Besides ZEB1, another EMT marker is the TIMP2, which is involved in the suppression

of matrix metalloproteinase (MMP) activity and vascularization [39]. MiaPaCa2 and PaTuS cells had higher levels of *TIMP2* than PaTuT and Panc01 cells, suggesting these to be vulnerable to cellular outgrowth. Indeed, PaTuT showed more ZEB1 and vimentin expression than PaTuS cells. Also, other markers that are associated with the mesenchymal-like phenotype, such as αSMA, were not changed due to the treatment. These data suggest that plasma treatment was not promoting EMT and metastatic potential of human pancreatic cancer cells *in vitro* and *in ovo*. Even more, tumor cells with a more mesenchymal profile, such as Panc01, were particularly sensitive to plasma treatment in terms of reduced outgrowth, as seen in tumor spheroid experiments. In general, spheroids are utilized in several studies utilizing plasma treatments, while most of them are using plasma-oxidized media or lacked an additional extracellular matrix so that no outgrowth was monitored, but showed a strong reduction in the growth of these 3D-models [23, 28, 34, 69–76].

The inflammatory profile in the tumor microenvironment—especially regarding the crosstalk with stromal cells—is decisive in tumor metastasis ever since the discovery of the link between chronic inflammation and tumorigenesis by Rudolf Virchow in 1863 [77–79]. However, the specific traits of inflammation are as heterogeneous as are different tumor types and stages [80], but some universal findings include the pro-angiogenic property of TGFβ and VEGF [81]. While *in vitro* changes in both molecules were rather modest, we identified an increase in VEGF with plasma treatment *in ovo* with PaTuS and PaTuT, while VEGF was decreased in MiaPaCa2 and Panc01. It has to be stated, however, that the origin of targets measured in samples from *in ovo* experiments cannot be explicitly determined (due to, e.g., angiogenesis provided by the chicken embryo as well). Noteworthy, none of the 13 molecules investigated followed the same tendency after plasma treatment, neither *in vitro* nor *in ovo*. By contrast, for each cell line, there were clear and consistent patterns. For Panc01, the majority of targets were either similar or markedly decreased, especially *in vitro*. This supports other findings of this study, pointing to cellular senescence. This pathway has been recently unraveled in Panc01 cells, with miR-137 as a central switch [82] that may have also been activated with plasma treatment but warrants further studies. PaTuS and PaTuT, two sister cell lines with different metastatic potential, showed a similar regulation of chemokines and cytokines release (especially IL6, IL8, CXCL1, and VEGF) despite their different sensitivity to plasma treatment. VEGF production may be a consequence of hypoxia-inducible factor 1α (HIF1α) activation with IL8 serving as another molecule to support angiogenesis [83] and tumor growth [84]. By contrast, IL8 also is positively associated with oxidative immunogenic cancer cell death (ICD) in melanoma cells, together with the activation of dendritic cells [85]. This was similar to the increased levels of IL6 in that study. IL6 is a potent attractor of monocytes/macrophages [86], which can, in turn, be supportive or detrimental for tumor growth, depending on microenvironmental factors [87]. Being the ligand for CXCR2 [88] and a neutrophil chemoattractant [89], CXCL1 is associated with poor prognosis in cancer due to its growth-stimulating, pro-angiogenic properties [90], also in pancreatic cancer [91], by encouraging tumor-stromal interactions. Increased levels

of this chemokine were found in PaTuS and PaTuT cells, which at least for PaTuS might explain the different tissue morphology observed for E-cadherin compared to that of PaTuS. Also, an increased release of IFNγ and TNFα was identified following plasma treatment. Both molecules were previously linked to antiproliferative effects in pancreatic cancer cells [92].

CONCLUSION

The results provide valuable insights into the effect of plasma treatment on metastasis-related properties of cancer cells *in vitro* and *in ovo* and did not suggest EMT-promoting effects of this novel cancer therapy. For future research, a detailed investigation of the EMT modulation through specific reactive species should be carried out. Although being technically challenging, future studies using *in vivo* models on cancer metastasis after plasma treatment are needed to validate our findings and the investigations should be extended to other tumor fields and clinical applications also. In addition, plasma treatment should be combined with existing therapies to identify its adjuvant potential.

DATA AVAILABILITY STATEMENT

The raw data supporting the conclusions of this article will be made available by the authors, without undue reservation.

ETHICS STATEMENT

Ethical review and approval was not required for the animal study because experiments with chicken embryos were terminated before day 15 from which on these experiments need to be declared to an ethics committee according to national regulations.

AUTHOR CONTRIBUTIONS

FUNDING

ACKNOWLEDGMENTS

REFERENCES

1. Bray F, Ferlay J, Soerjomataram I, Siegel RL, Torre LA, Jemal A. Global cancer statistics 2018: globocan estimates of incidence and mortality worldwide for 36 cancers in 185 countries. *CA Cancer J. Clin.* (2018) **68**:394–424. doi: 10.3322/caac.21492

2. Ledford H, Else H, Warren M. Cancer immunologists scoop medicine nobel prize. *Nature.* (2018) **562**:20–1. doi: 10.1038/d41586-018-06751-0

3. Delyon J, Lebbe C, Dumaz N. Targeted therapies in melanoma beyond BRAF: targeting NRAS-mutated and KIT-mutated melanoma. *Curr Opin Oncol.* (2020) **32**:79–84. doi: 10.1097/CCO.0000000000000606

4. Domenichini A, Adamska A, Falasca M. Abc transporters as cancer drivers: potential functions in cancer development. *Biochim Biophys Acta Gen Subj.* (2019) **1863**:52–60. doi: 10.1016/j.bbagen.2018.09.019

5. Gondivkar SM, Gadbail AR, Choudhary MG, Vedpathak PR, Likhitkar MS. Photodynamic treatment outcomes of potentially-malignant lesions and malignancies of the head and neck region: a systematic review. *J. Investig. Clin. Dent.* (2018) **9**:e12270. doi: 10.1111/jicd.12270

6. Pinto A, Pocard M. Photodynamic therapy and photothermal therapy for the treatment of peritoneal metastasis: a systematic review. *Pleura Peritoneum.* (2018) **3**:20180124. doi: 10.1515/pp-2018-0124

7. Privat-Maldonado A, Schmidt A, Lin A, Weltmann KD, Wende K, Bogaerts A, et al. ROS from physical plasmas: redox chemistry for biomedical therapy. *Oxid. Med. Cell. Longev.* (2019) **2019**:9062098. doi: 10.1155/2019/9062098

8. von Woedtke T, Schmidt A, Bekeschus S, Wende K, Weltmann KD. Plasma medicine: a field of applied redox biology. *In Vivo.* (2019) **33**:1011–26. doi: 10.21873/invivo.11570

9. von Woedtke T, Schmidt A, Bekeschus S, Wende K. Introduction to plasma medicine. In: Metelmann H-R, von Woedtke T, Weltmann K-D, editors. *Comprehensive Clinical Plasma Medicine.* Cham: Springer International Publishing (2018). p. 3–21. doi: 10.1007/978-3-319-67627-2_1

10. Metelmann H-R, Seebauer C, Miller V, Fridman A, Bauer G, Graves DB, et al. Clinical experience with cold plasma in the treatment of locally advanced head and neck cancer. *Clin. Plas. Med.* (2018) **9**:6–13. doi: 10.1016/j.cpme.2017.09.001

11. Witzke K, Seebauer C, Jesse K, Kwiatek E, Berner J, Semmler M-L, et al. Plasma medical oncology: immunological interpretation of head and neck squamous cell carcinoma. *Plasma Process. Polym.* (2020). doi: 10.1002/ppap.201900258. [Epub ahead of print].

12. Hanahan D, Weinberg RA. Hallmarks of cancer: the next generation. *Cell.* (2011) **144**:646–74. doi: 10.1016/j.cell.2011.02.013

13. Mantovani A, Marchesi F, Malesci A, Laghi L, Allavena P. Tumour-associated macrophages as treatment targets in oncology. *Nat. Rev. Clin. Oncol.* (2017) **14**:399–416. doi: 10.1038/nrclinonc.2016.217

14. Tuting T, de Visser KE. Cancer. How neutrophils promote metastasis. *Science.* (2016) **352**:145–6. doi: 10.1126/science.aaf7300

15. Guan X. Cancer metastases: challenges and opportunities. *Acta Pharm Sin B.* (2015) **5**:402–18. doi: 10.1016/j.apsb.2015.07.005

16. Klaiber U, Schnaidt ES, Hinz U, Gaida MM, Heger U, Hank T, et al. Prognostic factors of survival after neoadjuvant treatment and resection for initially unresectable pancreatic cancer. *Ann. Surg.* (2019). doi: 10.1097/SLA.0000000000003270. [Epub ahead of print].

17. Mahajan UM, Langhoff E, Goni E, Costello E, Greenhalf W, Halloran C, et al. Immune cell and stromal signature associated with progression-free survival of patients with resected pancreatic ductal adenocarcinoma. *Gastroenterology.* (2018) **155**:1625–39.e1622. doi: 10.1053/j.gastro.2018.08.009

18. Krebs AM, Mitschke J, Lasierra Losada M, Schmalhofer O, Boerries M, Busch H, et al. The emt-activator zeb1 is a key factor for cell plasticity and promotes metastasis in pancreatic cancer. *Nat. Cell Biol.* (2017) **19**:518–29. doi: 10.1038/ncb3513

19. Granata V, Fusco R, Setola SV, Piccirillo M, Leongito M, Palaia R, et al. Early radiological assessment of locally advanced pancreatic cancer treated with electrochemotherapy. *World J. Gastroenterol.* (2017) **23**:4767–78. doi: 10.3748/wjg.v23.i26.4767

20. Jayson GC, Kerbel R, Ellis LM, Harris AL. Antiangiogenic therapy in oncology: current status and future directions. *Lancet.* (2016) **388**:518–29. doi: 10.1016/S0140-6736(15)01088-0

21. Tafuto S, von Arx C, De Divitiis C, Maura CT, Palaia R, Albino V, et al. Electrochemotherapy as a new approach on pancreatic cancer and on liver metastases. *Int. J. Surg.* (2015) **21**(Suppl. 1):S78–82. doi: 10.1016/j.ijsu.2015.04.095

22. Zheng X, Carstens JL, Kim J, Scheible M, Kaye J, Sugimoto H, et al. Epithelial-to-mesenchymal transition is dispensable for metastasis but induces chemoresistance in pancreatic cancer. *Nature.* (2015) **527**:525–30. doi: 10.1038/nature16064

23. Freund E, Liedtke KR, van der Linde J, Metelmann HR, Heidecke CD, Partecke LI, et al. Physical plasma-treated saline promotes an immunogenic phenotype in ct26 colon cancer cells *in vitro* and *in vivo*. *Sci. Rep.* (2019) **9**:634. doi: 10.1038/s41598-018-37169-3

24. Wende K, Schmidt A, Bekeschus S. Safety aspects of non-thermal plasmas. In: Metelmann H-R, von Woedtke T, Weltmann K-D, editors. *Comprehensive Clinical Plasma Medicine.* Cham: Springer International Publishing (2018). p. 83–109. doi: 10.1007/978-3-319-67627-2_5

25. Bekeschus S, Schmidt A, Kramer A, Metelmann HR, Adler F, von Woedtke T, et al. High throughput image cytometry micronucleus assay to investigate the presence or absence of mutagenic effects of cold physical plasma. *Environ. Mol. Mutagen.* (2018) **59**:268–77. doi: 10.1002/em.22172

26. Schmidt A, Woedtke TV, Stenzel J, Lindner T, Polei S, Vollmar B, et al. One year follow-up risk assessment in SKH-1 mice and wounds treated with an argon plasma jet. *Int. J. Mol. Sci.* (2017) **18**:868. doi: 10.3390/ijms18040868

27. Kluge S, Bekeschus S, Bender C, Benkhai H, Sckell A, Below H, et al. Investigating the mutagenicity of a cold argon-plasma jet in an het-mn model. *PLoS ONE.* (2016) **11**:e0160667. doi: 10.1371/journal.pone.0160667

28. Bekeschus S, Freund E, Spadola C, Privat-Maldonado A, Hackbarth C, Bogaerts A, et al. Risk assessment of kinpen plasma treatment of four human pancreatic cancer cell lines with respect to metastasis. *Cancers.* (2019) **11**:1237. doi: 10.3390/cancers11091237

29. Lademann J, Ulrich C, Patzelt A, Richter H, Kluschke F, Klebes M, et al. Risk assessment of the application of tissue-tolerable plasma on human skin. *Clin. Plas. Med.* (2013) **1**:5–10. doi: 10.1016/j.cpme.2013.01.001

30. Daeschlein G, Scholz S, Ahmed R, Majumdar A, von Woedtke T, Haase H. et al. Cold plasma is well-tolerated and does not disturb skin barrier or reduce skin moisture. *J Dtsch Dermatol Ges.* (2012) **10**:509–15. doi: 10.1111/j.1610-0387.2012.07857.x

31. Metelmann H-R, Vu TT, Do HT, Le TNB, Hoang THA, Phi TTT, et al. Scar formation of laser skin lesions after cold atmospheric pressure plasma (cap) treatment: a clinical long term observation. *Clin. Plas. Med.* (2013) **1**:30–5. doi: 10.1016/j.cpme.2012.12.001

32. Schuster M, Rutkowski R, Hauschild A, Shojaei RK, von Woedtke T, Rana A, et al. Side effects in cold plasma treatment of advanced oral cancer—clinical data and biological interpretation. *Clin. Plas. Med.* (2018) **10**:9–15. doi: 10.1016/j.cpme.2018.04.001

33. Cramer GM, Jones DP, El-Hamidi H, Celli JP. Ecm composition and rheology regulate growth, motility, and response to photodynamic therapy in 3D models of pancreatic ductal adenocarcinoma. *Mol. Cancer Res.* (2017) **15**:15–25. doi: 10.1158/1541-7786.MCR-16-0260

34. Privat-Maldonado A, Bengtson C, Razzokov J, Smits E, Bogaerts A. Modifying the tumour microenvironment: challenges and future perspectives for anticancer plasma treatments. *Cancers.* (2019) **11**:1920. doi: 10.3390/cancers11121920

35. Liao Z, Tan ZW, Zhu P, Tan NS. Cancer-associated fibroblasts in tumor microenvironment-accomplices in tumor malignancy. *Cell. Immunol.* (2018) **343**:103729. doi: 10.1016/j.cellimm.2017.12.003

36. Alonso-Nocelo M, Raimondo TM, Vining KH, Lopez-Lopez R, de la Fuente M, Mooney DJ. Matrix stiffness and tumor-associated macrophages modulate epithelial to mesenchymal transition of human adenocarcinoma cells. *Biofabrication.* (2018) **10**:035004. doi: 10.1088/1758-5090/aaafbc

37. Yilmaz M, Christofori G. EMT, the cytoskeleton, and cancer cell invasion. *Cancer Metastasis Rev.* (2009) **28**:15–33. doi: 10.1007/s10555-008-9169-0

38. Jesnowski R, Furst D, Ringel J, Chen Y, Schrodel A, Kleeff J, et al. Immortalization of pancreatic stellate cells as an *in vitro* model of pancreatic fibrosis: deactivation is induced by matrigel and n-acetylcysteine. *Lab. Invest.* (2005) **85**:1276–91. doi: 10.1038/labinvest.3700329

39. Seo D-W, Li H, Guedez L, Wingfield PT, Diaz T, Salloum R, et al. Timp-2 mediated inhibition of angiogenesis: an mmp-independent mechanism. *Cell.* (2003) **114**:171–80. doi: 10.1016/S0092-8674(03)00551-8

40. Collins A, Bloomston M. Diagnosis and management of pancreatic cancer. *Minerva Gastroenterol. Dietol.* (2009) **55**:445–54.

41. Ellenrieder V, Adler G, Gress TM. Invasion and metastasis in pancreatic cancer. *Ann. Oncol.* (1999) **10**:S46–50. doi: 10.1093/annonc/10.suppl_4.S46

42. Ghaneh P, Costello E, Neoptolemos JP. Biology and management of pancreatic cancer. *Postgrad. Med. J.* (2008) **84**:478–97. doi: 10.1136/gut.2006.103333

43. Flaum N, Hubner RA, Valle JW, Amir E, McNamara MG. Adjuvant chemotherapy and outcomes in patients with nodal and resection margin-negative pancreatic ductal adenocarcinoma: a systematic review and meta-analysis. *J. Surg. Oncol.* (2019) **119**:932–40. doi: 10.1002/jso.25440

44. Esposito I, Kleeff J, Bergmann F, Reiser C, Herpel E, Friess H, et al. Most pancreatic cancer resections are r1 resections. *Ann. Surg. Oncol.* (2008) **15**:1651–60. doi: 10.1245/s10434-008-9839-8

45. Bekeschus S, Kading A, Schroder T, Wende K, Hackbarth C, Liedtke KR, et al. Cold physical plasma-treated buffered saline solution as effective agent against pancreatic cancer cells. *Anticancer Agents Med. Chem.* (2018) **18**:824–31. doi: 10.2174/1871520618666180507130243

46. Liedtke KR, Diedrich S, Pati O, Freund E, Flieger R, Heidecke CD, et al. Cold physical plasma selectively elicits apoptosis in murine pancreatic cancer cells *in vitro* and *in ovo*. *Anticancer Res.* (2018) **38**:5655–63. doi: 10.21873/anticanres.12901

47. Masur K, von Behr M, Bekeschus S, Weltmann KD, Hackbarth C, Heidecke CD, et al. Synergistic inhibition of tumor cell proliferation by cold plasma and gemcitabine. *Plasma Process. Polym.* (2015) **12**:1377–82. doi: 10.1002/ppap.201500123

48. Yan D, Cui H, Zhu W, Nourmohammadi N, Milberg J, Zhang LG, et al. The specific vulnerabilities of cancer cells to the cold atmospheric plasma-stimulated solutions. *Sci. Rep.* (2017) **7**:4479. doi: 10.1038/s41598-017-04770-x

49. Hattori N, Yamada S, Torii K, Takeda S, Nakamura K, Tanaka H, et al. Effectiveness of plasma treatment on pancreatic cancer cells. *Int. J. Oncol.* (2015) **47**:1655–62. doi: 10.3892/ijo.2015.3149

50. Liedtke KR, Bekeschus S, Kaeding A, Hackbarth C, Kuehn JP, Heidecke CD, et al. Non-thermal plasma-treated solution demonstrates antitumor activity against pancreatic cancer cells *in vitro* and *in vivo*. *Sci. Rep.* (2017) **7**:8319. doi: 10.1038/s41598-017-08560-3

51. Sato Y, Yamada S, Takeda S, Hattori N, Nakamura K, Tanaka H, et al. Effect of plasma-activated lactated ringer's solution on pancreatic cancer cells *in vitro* and *in vivo*. *Ann. Surg. Oncol.* (2018) **25**:299–307. doi: 10.1245/s10434-017-6239-y

52. Partecke LI, Evert K, Haugk J, Doering F, Normann L, Diedrich S, et al. Tissue tolerable plasma (ttp) induces apoptosis in pancreatic cancer cells *in vitro* and *in vivo*. *BMC Cancer.* (2012) **12**:473. doi: 10.1186/1471-2407-12-473

53. Stoffels E, Kieft IE, Sladek REJ, van den Bedem LJM, van der Laan EP, Steinbuch M. Plasma needle for *in vivo* medical treatment: recent developments and perspectives. *Plasma Sources Sci. T.* (2006) **15**:S169–80. doi: 10.1088/0963-0252/15/4/S03

54. Stoffels E, Roks AJM, Deelmm LE. Delayed effects of cold atmospheric plasma on vascular cells. *Plasma Process. Polym.* (2008) **5**:599–605. doi: 10.1002/ppap.200800028

55. Stoffels E, Sakiyama Y, Graves DB. Cold atmospheric plasma: charged species and their interactions with cells and tissues. *IEEE Trans. Plasma Sci.* (2008) **36**:1441–57. doi: 10.1109/TPS.2008.2001084

56. Ribatti D. The chick embryo chorioallantoic membrane (cam). A multifaceted experimental model. *Mech. Dev.* (2016) **141**:70–7. doi: 10.1016/j.mod.2016.05.003

57. Izard T, Brown DT. Mechanisms and functions of vinculin interactions with phospholipids at cell adhesion sites. *J. Biol. Chem.* (2016) **291**:2548–55. doi: 10.1074/jbc.R115.686493

58. Shih HP, Panlasigui D, Cirulli V, Sander M. ECM signaling regulates collective cellular dynamics to control pancreas branching morphogenesis. *Cell Rep.* (2016) **14**:169–79. doi: 10.1016/j.celrep.2015.12.027

59. Beachley VZ, Wolf MT, Sadtler K, Manda SS, Jacobs H, Blatchley MR, et al. Tissue matrix arrays for high-throughput screening and systems analysis of cell function. *Nat. Methods.* (2015) **12**:1197–204. doi: 10.1038/nmeth.3619

60. Grzesiak JJ, Ho JC, Moossa AR, Bouvet M. The integrin-extracellular matrix axis in pancreatic cancer. *Pancreas.* (2007) **35**:293–301. doi: 10.1097/mpa.0b013e31811f4526

61. Ni J, Cozzi PJ, Duan W, Shigdar S, Graham PH, John KH, et al. Role of the EpCAM (CD326) in prostate cancer metastasis and progression. *Cancer Metastasis Rev.* (2012) **31**:779–91. doi: 10.1007/s10555-012-9389-1

62. Munz M, Baeuerle PA, Gires O. The emerging role of epcam in cancer and stem cell signaling. *Cancer Res.* (2009) **69**:5627. doi: 10.1158/0008-5472.CAN-09-0654

63. Baeuerle PA, Gires O. EpCAM (CD326) finding its role in cancer. *Br. J. Cancer.* (2007) **96**:417–23. doi: 10.1038/sj.bjc.6603494

64. Canel M, Serrels A, Frame MC, Brunton VG. E-cadherin-integrin crosstalk in cancer invasion and metastasis. *J. Cell Sci.* (2013) **126**:393–401. doi: 10.1242/jcs.100115

65. Spaderna S, Schmalhofer O, Wahlbuhl M, Dimmler A, Bauer K, Sultan A, et al. The transcriptional repressor ZEB1 promotes metastasis and loss of cell polarity in cancer. *Cancer Res.* (2008) **68**:537–44. doi: 10.1158/0008-5472.CAN-07-5682

66. Wellner U, Brabletz T, Keck T. Zeb1 in pancreatic cancer. *Cancers.* (2010) **2**:1617–28. doi: 10.3390/cancers2031617

67. Kurahara H, Takao S, Maemura K, Mataki Y, Kuwahata T, Maeda K, et al. Epithelial–mesenchymal transition and mesenchymal–epithelial transition via regulation of ZEB-1 and ZEB-2 expression in pancreatic cancer. *J. Surg. Oncol.* (2012) **105**:655–61. doi: 10.1002/jso.23020

68. Zhang GJ, Zhou T, Tian HP, Liu ZL, Xia SS. High expression of ZEB1 correlates with liver metastasis and poor prognosis in colorectal cancer. *Oncol. Lett.* (2013) **5**:564–68. doi: 10.3892/ol.2012.1026

69. Judee F, Fongia C, Ducommun B, Yousfi M, Lobjois V, Merbahi N. Short and long time effects of low temperature plasma activated media on 3D multicellular tumor spheroids. *Sci. Rep.* (2016) **6**:21421. doi: 10.1038/srep21421

70. Chauvin J, Gibot L, Griseti E, Golzio M, Rols MP, Merbahi N, et al. Elucidation of *in vitro* cellular steps induced by antitumor treatment with plasma-activated medium. *Sci. Rep.* (2019) **9**:4866. doi: 10.1038/s41598-019-41408-6

71. Gandhirajan RK, Rodder K, Bodnar Y, Pasqual-Melo G, Emmert S, Griguer CE, et al. Cytochrome C oxidase inhibition and cold plasma-derived oxidants synergize in melanoma cell death induction. *Sci. Rep.* (2018) **8**:12734. doi: 10.1038/s41598-018-31031-2

72. Sagwal SK, Pasqual-Melo G, Bodnar Y, Gandhirajan RK, Bekeschus S. Combination of chemotherapy and physical plasma elicits melanoma cell death via upregulation of SLC22A16. *Cell Death Dis.* (2018) **9**:1179. doi: 10.1038/s41419-018-1221-6

73. Privat-Maldonado A, Gorbanev Y, Dewilde S, Smits E, Bogaerts A. Reduction of human glioblastoma spheroids using cold atmospheric plasma: the combined effect of short- and long-lived reactive species. *Cancers.* (2018) **10**:394. doi: 10.3390/cancers10110394

74. Beaumont KA, Mohana-Kumaran N, Haass NK. Modeling melanoma *in vitro* and *in vivo*. *Healthcare.* (2013) **2**:27–46. doi: 10.3390/healthcare2010027

75. Griseti E, Kolosnjaj-Tabi J, Gibot L, Fourquaux I, Rols MP, Yousfi M, et al. Pulsed electric field treatment enhances the cytotoxicity of plasma-activated liquids in a three-dimensional human colorectal cancer cell model. *Sci. Rep.* (2019) **9**:7583. doi: 10.1038/s41598-019-44087-5

76. Freund E, Liedtke KR, Miebach L, Wende K, Heidecke A, Kaushik NK, et al. Identification of two kinase inhibitors with synergistic toxicity with low-dose hydrogen peroxide in colorectal cancer cells *in vitro*. *Cancers.* (2020) **12**:122. doi: 10.3390/cancers12010122

77. Balkwill F, Mantovani A. Inflammation and cancer: back to virchow? *Lancet.* (2001) **357**:539–45. doi: 10.1016/S0140-6736(00)04046-0

78. Coussens LM, Werb Z. Inflammation and cancer. *Nature.* (2002) **420**:860–7. doi: 10.1038/nature01322

79. Steele CW, Jamieson NB, Evans TR, McKay CJ, Sansom OJ, Morton JP, et al. Exploiting inflammation for therapeutic gain in pancreatic cancer. *Br. J. Cancer.* (2013) **108**:997–1003. doi: 10.1038/bjc.2013.24

80. Savant SS, Sriramkumar S, O'Hagan HM. The role of inflammation and inflammatory mediators in the development, progression, metastasis,

and chemoresistance of epithelial ovarian cancer. *Cancers.* (2018) **10**:251. doi: 10.3390/cancers10080251

81. Quail DF, Joyce JA. Microenvironmental regulation of tumor progression and metastasis. *Nat. Med.* (2013) **19**:1423–37. doi: 10.1038/nm.3394

82. Neault M, Mallette FA, Richard S. miR-137 modulates a tumor suppressor network-inducing senescence in pancreatic cancer cells. *Cell Rep.* (2016) **14**:1966–78. doi: 10.1016/j.celrep.2016.01.068

83. Mizukami Y, Jo WS, Duerr EM, Gala M, Li J, Zhang X, et al. Induction of interleukin-8 preserves the angiogenic response in hif-1alpha-deficient colon cancer cells. *Nat. Med.* (2005) **11**:992–7. doi: 10.1038/nm1294

84. Garofalo M, Iovine B, Kuryk L, Capasso C, Hirvinen M, Vitale A, et al. Oncolytic adenovirus loaded with l-carnosine as novel strategy to enhance the antitumor activity. *Mol. Cancer Ther.* (2016) **15**:651–60. doi: 10.1158/1535-7163.MCT-15-0559

85. Dudek-Peric AM, Ferreira GB, Muchowicz A, Wouters J, Prada N, Martin S, et al. Antitumor immunity triggered by melphalan is potentiated by melanoma cell surface-associated calreticulin. *Cancer Res.* (2015) **75**:1603–14. doi: 10.1158/0008-5472.CAN-14-2089

86. Clahsen T, Schaper F. Interleukin-6 acts in the fashion of a classical chemokine on monocytic cells by inducing integrin activation, cell adhesion, actin polymerization, chemotaxis, and transmigration. *J. Leukoc. Biol.* (2008) **84**:1521–9. doi: 10.1189/jlb.0308178

87. Najafi M, Hashemi Goradel N, Farhood B, Salehi E, Nashtaei MS, Khanlarkhani N, et al. Macrophage polarity in cancer: a review. *J. Cell. Biochem.* (2019) **120**:2756–65. doi: 10.1002/jcb.27646

88. Tsai H-H, Frost E, To V, Robinson S, ffrench-Constant C, Geertman R, et al. The chemokine receptor CXCR2 controls positioning of oligodendrocyte precursors in developing spinal cord by arresting their migration. *Cell.* (2002) **110**:373–83. doi: 10.1016/S0092-8674(02)00838-3

89. De Filippo K, Dudeck A, Hasenberg M, Nye E, van Rooijen N, Hartmann K, et al. Mast cell and macrophage chemokines CXCL1/CXCL2 control the early stage of neutrophil recruitment during tissue inflammation. *Blood.* (2013) **121**:4930–7. doi: 10.1182/blood-2013-02-486217

90. Acharyya S, Oskarsson T, Vanharanta S, Malladi S, Kim J, Morris PG, et al. A CXCL1 paracrine network links cancer chemoresistance and metastasis. *Cell.* (2012) **150**:165–78. doi: 10.1016/j.cell.2012.04.042

91. Ijichi H, Chytil A, Gorska AE, Aakre ME, Bierie B, Tada M, et al. Inhibiting CXCR2 disrupts tumor-stromal interactions and improves survival in a mouse model of pancreatic ductal adenocarcinoma. *J. Clin. Invest.* (2011) **121**:4106–17. doi: 10.1172/JCI42754

92. Schmiegel WH, Caesar J, Kalthoff H, Greten H, Schreiber HW, Thiele HG. Antiproliferative effects exerted by recombinant human tumor necrosis factor-alpha (tnf-alpha) and interferon-gamma (ifn-gamma) on human pancreatic tumor cell lines. *Pancreas.* (1988) **3**:180–8. doi: 10.1097/00006676-198804000-00012